SSIM 2025 - JJ Potter & J Wesseloo (eds)

doi:10.36487/ACG_repo/2535_51

Simulated 3D slope stability monitoring using InSAR enabled by the MDA CHORUS synthetic aperture radar constellation

Dylan Hickson [a,*], Peter Oliver [a], Roger Morin [a]

[a] *MDA Space, Canada*

Abstract

Satellite synthetic aperture radar (SAR) observations are crucial for an effective ground stability monitoring program in mining operations. Interferometric processing can provide millimetre-precision time series measurements of ground displacement at high resolution over wide areas, regardless of time of day or weather conditions. However, if the direction of ground displacement is not aligned with the line-of-sight (LOS) between the satellite and target, the measurements will be significantly underestimated. Furthermore, the side-looking imaging geometry of these satellites introduces imaging distortions, such as layover and shadow, that also depend on the LOS and surface topography. These limitations on the quality of interferometric measurements are significant over mining sites with complex topographies and dynamic ground movement. These disadvantages can be partially overcome by incorporating multiple imaging geometries into the monitoring plan; however, given that most SAR satellites are sun-synchronous orbiting (SSO), a nearly polar orbit, this only improves sensitivity to east–west components of ground motion, leaving any north–south components poorly constrained.

MDA Space will soon be offering MDA CHORUS, a next-generation dual-frequency C- and X-band SAR satellite constellation which will operate in an innovative mid-inclination orbit that provides access to new imaging geometries for interferometric processing. These unique LOS vectors will increase the measurement coverage in areas with variable topography and enable 3D ground displacement measurements with high precision in all directions, including the north–south component.

In this work we present simulations of InSAR processing for 3D ground displacement monitoring at the Betze-Post open pit at the Goldstrike mine in Nevada, USA. For the open pit we show how measurements by CHORUS increase the density of reliable measurements for a better characterisation of ground motion. For various multi-sensor combinations of CHORUS with SSO SAR sensors, such as CHORUS and RADARSAT-2, we simulate the precision attainable in 3D ground displacement measurements.

Keywords: *slope stability, subsidence, geotechnical risk, remote sensing, InSAR*

1 Introduction

Remote sensing can provide unique, valuable information to mine sites that is not available with conventional in situ instrumentation and is increasingly being integrated into geotechnical monitoring programs. The active microwave radiation used by satellite synthetic aperture radar (SAR) sensors allows for imaging to occur at day or night and can penetrate through most weather conditions, allowing for high-resolution images to be acquired over large areas. Furthermore, spaceborne sensors provide predictable, repeated imaging over long periods of time, which allows information derived from the analysis of SAR data to be reliably incorporated into geotechnical monitoring programs.

Interferometric SAR (InSAR) exploits the coherent nature of SAR signals to detect and measure millimetre-scale surface displacements. From a pair of SAR images collected at different times, the phase difference is calculated

[*] Corresponding author. Email address: Dylan.Hickson@mda.space

on a per-pixel basis. After modelling and removing various phase contributions, this phase difference is directly proportional to the ground deformation which occurred along the SAR line-of-sight (LOS) in the time between collection of the first and second SAR images. This phase differencing approach allows for the detection and measurement of deformation much smaller than the radar wavelength. Under correct circumstances, InSAR allows for the surveillance of broader areas for more subtle deformation than conventional monitoring, without the need for sending workers into the field to install in situ instrumentation.

MDA Space will soon be offering CHORUS, a next-generation dual-frequency C- and X-band SAR satellite constellation that will have an innovative mid-inclination orbit (Sharma et al. 2022, 2024; Eppler et al. 2023; Greene Gondi et al. 2023). The benefits of the unique viewing geometries offered by this mid-inclination orbit have been theorised as early as 2004 (Wright et al. 2004); the variety of LOS vectors will better constrain InSAR analyses to reduce bias in the magnitude of measured surface displacement and resolve the 3D orientation of ground movement. Similarly, in areas of complex topography where SAR distortions can obscure coverage from sun-synchronous orbiting (SSO) SAR sensors with limited viewing geometries, incorporating CHORUS can allow for previously unobserved pixels to be illuminated for the first time.

In this work, the results of simulations illustrating InSAR coverage and expected 3D InSAR surface displacement measurement for the Betze-Post open pit at the Goldstrike mine in Nevada, USA, are presented. Background information describing the measurement of 3D surface displacement with InSAR, as well as geometric distortions limiting the coverage, is presented. Finally, the simulation results are presented and discussed in terms of their implications for InSAR monitoring programs at mine sites.

1.1 Background

In this section, the concepts required to understand the limitations of InSAR measurements in the context of this study are described.

1.1.1 3D interferometric synthetic aperture radar geometry

Repeat-pass InSAR measures a projection of surface displacement onto the SAR LOS. Unless the SAR LOS is perfectly aligned with the surface displacement vector, which is generally not the case, then the displacement measurement using a single SAR LOS will be underestimated. This is depicted in Figure 1 (Greene Gondi et al. 2023; Brouwer & Hanssen 2023), where θ is the incidence angle from the target to the SAR sensor and α_d is the azimuth of the zero Doppler plane from the target towards the SAR sensor.

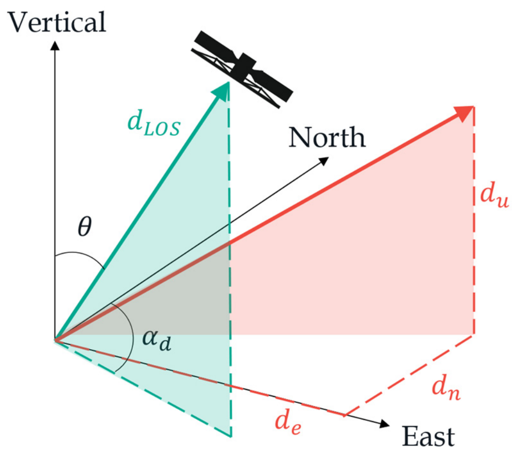

Figure 1 3D InSAR geometry with synthetic aperture radar line-of-sight

In circumstances where a priori knowledge can constrain the expected surface displacement to one direction, e.g. assuming vertical deformation only for an area of known subsidence, then LOS InSAR observations are commonly projected onto the vertical plane. This results in a measurement that is easy to interpret but, if any horizontal deformation was present, there would be substantial error in the vertical deformation estimates, especially for shallow incidence angles (Furhmann & Garthwaite 2019).

When InSAR observations from multiple LOS are available, this idea can be expanded to recover the full 3D surface displacement vector. The process of inverting a set of LOS InSAR measurements to compute the 3D components of the measured surface displacement is termed '3D decomposition' and described in detail in Brouwer & Hanssen (2023) and Greene Gondi et al. (2023). The accuracy of the 3D decomposition is related to the angular diversity of InSAR LOS vectors used, where the limited viewing geometries of current SSO SAR sensors results in poor reconstruction of horizontal displacement in the north–south plane (Wright et al. 2004; Greene Gondi et al. 2023). SSO SAR sensors, operating in a nearly polar orbit and looking orthogonal to the flight direction, have LOS aligned with the east–west plane. This results in relatively low angular diversity, even when observations from opposing radar look and satellite pass directions are combined. When combinations of SSO InSAR LOS measurements are decomposed, the low angular diversity results in a highly unstable solution sensitive to measurement noise, which effectively prevents any measurement of north–south deformation. These errors can significantly impact the geotechnical interpretation of the InSAR measurements in assessing the amount of ground movement.

1.1.2 Synthetic aperture radar image distortions

Satellite SAR sensors collect imagery from side-looking geometries, which introduces distortions on topographic features; the severity of which depends on the incidence angle. These distortions present challenges when geocoding and subsequently interpreting SAR images, and also impact InSAR analyses. The relevant SAR image distortions, i.e. 'layover', 'foreshortening' and 'shadow', each of which can impact InSAR analyses, are illustrated in Figure 2 and elaborated on below.

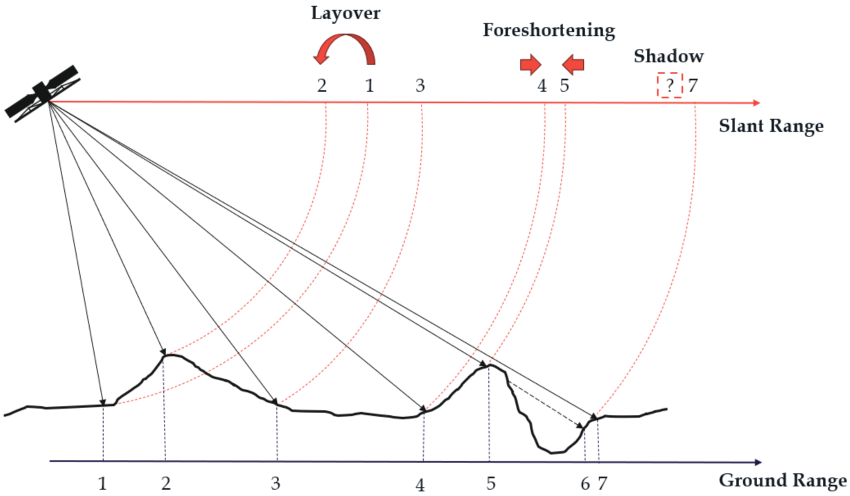

Figure 2 Synthetic aperture radar image distortions between slant range and ground range for different surface topographies

On steep slopes facing the SAR sensor the signal is scattered back to the radar from the top of the slope before the bottom. This situation, termed 'layover', causes the tops of steep slopes to appear at an earlier slant range than the bottom of the slope. In Figure 2 this results in point 2 being imaged before point 1. For slopes facing the SAR sensor that are less steep, the top of the slope is imaged sooner than if the terrain was flat. This situation, termed 'foreshortening', causes slopes to appear compressed in the SAR image. In Figure 2 this results in points 4 and 5 appearing closer together in slant range compared to their ground range distance. The LOS to targets on slopes oriented away from the sensor can be obstructed by surrounding topography. In this situation, termed 'shadow', these targets are not illuminated by the sensor at all and are not present in slant range. In Figure 2 this results in point 6 missing from the slant range projection and not being imaged by the SAR sensor. The SAR distortions described above mix the radar backscatter from several geographic positions and cannot be used in an InSAR analysis.

1.2 The CHORUS mission

The CHORUS SAR constellation, currently targeted for launch in mid-2026, comprises two satellites, a C-band SAR (CHORUS-C) built by MDA Space and an X-band SAR (CHORUS-X) supplied by ICEYE for the exclusive use of MDA Space. CHORUS-C and CHORUS-X will offer left- or right-looking imaging modes between 24.5° and 63.9° incidence. This results in coverage between ± 62.5° latitude (89% global access) and an accessible swathe of 700 km. Both satellites will maintain an orbital tube sufficient for interferometric exploitation for optimal imaging and results. CHORUS will provide high quality repeat-pass InSAR for deformation monitoring with a repeat cycle of 9.85 days. The reader is referred to Sharma et al. (2024) for additional details on the CHORUS mission. Table 1 describes the orbit parameters for the CHORUS mission (Sharma et al. 2024; Greene Gondi et al. 2023).

Table 1 CHORUS orbit parameters

Orbit parameter	Value
Type	Mid-inclination, non sun-synchronous
Altitude	~600 km
Inclination	53.5° (prograde)
Repeat cycle	9.85 days (147 orbits)
Phasing	Same ground track, CHORUS-X trails CHORUS-C by 1 hour
Orbit control	Maintained in an orbital tube suitable for repeat-pass interferometry

2 Methodology

In this section we describe the area of interest (AOI) analysed in this study and the simulations performed.

2.1 Area of interest

The Goldstrike Mine Complex is one of the largest gold mining operations in the US. Each year millions of ounces of gold are extracted from a belt of gold deposits within the Carlin Trend, a geologic feature about 8.0 km wide and 64 km long. The mining complex consists of three separate mines. The largest open pit, the Betze-Post pit, is located at the northern end of the Carlin Trend and is the focus of the analysis for this study. To characterise the complex topography within the AOI, a digital elevation model (DEM) with 1 m resolution was used. This DEM is shown, hillshaded with an azimuth of 315° and altitude of 45°, in Figure 3.

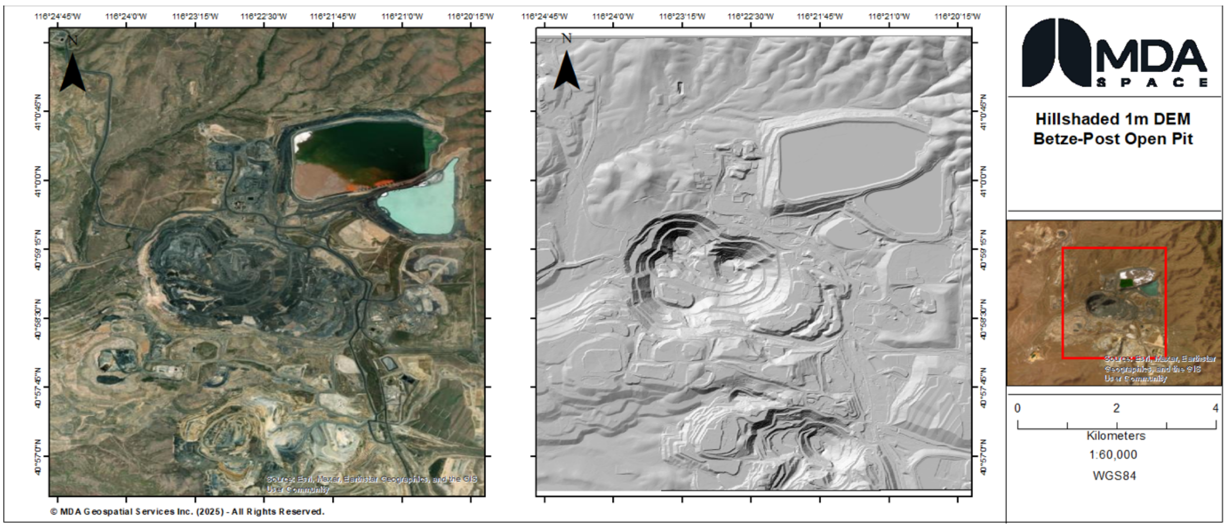

Figure 3 Optical image and hillshaded 1 m digital elevation model (DEM) for the Betze-Post open pit

2.2 SAR dataset optimisation

Both RADARSAT-2 and CHORUS offer a variety of imaging geometries and beam modes, which results in many potential LOS combinations to perform 3D decomposition. However, only ideal combinations of these imaging geometries (i.e. those with suitably large angular variety in their LOS) will result in improved 3D decomposition performance relative to using SSO sensors only. To determine the ideal combinations for 3D decomposition, an optimisation procedure was developed. The optimisation presented here only considers how the imaging geometry provides sensitivity to 3D components of surface motion. We consider all possible incidence angles to inspect the full range of potential imaging geometries. A more detailed analysis that incorporates additional factors, such as backscatter and phase noise variation among imaging geometries, will be the focus of future work.

To illustrate the limited angular diversity available from many existing SSO SAR sensors, we considered five possible stacks of archived RADARSAT-2 Ultrafine images collected in right-looking ascending and descending orbits. We considered 23 simulated CHORUS 3 m resolution Stripmap beam mode left- and right-looking image stacks available within 137 ascending and descending orbits to examine how these geometries improved the angular diversity for 3D decomposition. This large set of available data results in many potential combinations for 3D decomposition; for this set of 28 independent image stacks, there are 3,726 combinations of three stacks. If allowing for combinations of four or more beams, the number of combinations increases further.

To demonstrate the improvement in performance when introducing CHORUS, the optimisation was performed twice: first including only the 5 RADARSAT-2 Ultrafine images, and a second time including all 28 RADARSAT-2 and CHORUS stacks. The results of this are two cases. The first scenario, ‘Case 1’, considers the three RADARSAT-2 beams only, which represents the 3D InSAR capabilities of SSO SAR sensors. The second scenario, ‘Case 2’, considers the optimal combination of RADARSAT-2 and CHORUS-C beams to provide the best precision in 3D decomposition of LOS InSAR surface displacement measurements. Table 2 describes the beam modes considered for Cases 1 and 2.

Table 2 RADARSAT-2 and CHORUS-C beam modes considered in the simulation

Beam identifier	SAR satellite	Beam mode	Orbit direction	Look direction	Incidence angle	Beam heading	Simulation ID
U4W2DR	RADARSAT-2	Ultrafine	Descending	Right	33.00°	191°	Case 1
U22W2AR	RADARSAT-2	Ultrafine	Ascending	Right	46.01°	351°	Case 1
U23W2DR	RADARSAT-2	Ultrafine	Descending	Right	46.65°	189°	Case 1
U16W2DR	RADARSAT-2	Ultrafine	Descending	Right	42.1°	190°	Case 2
ST3m015AR	CHORUS-C	Stripmap	Ascending	Right	51°	60°	Case 2
ST3m025DL	CHORUS-C	Stripmap	Descending	Left	62°	140°	Case 2

The areas imaged by each beam under consideration are shown in Figure 4 below, with the two cases differentiated by line style.

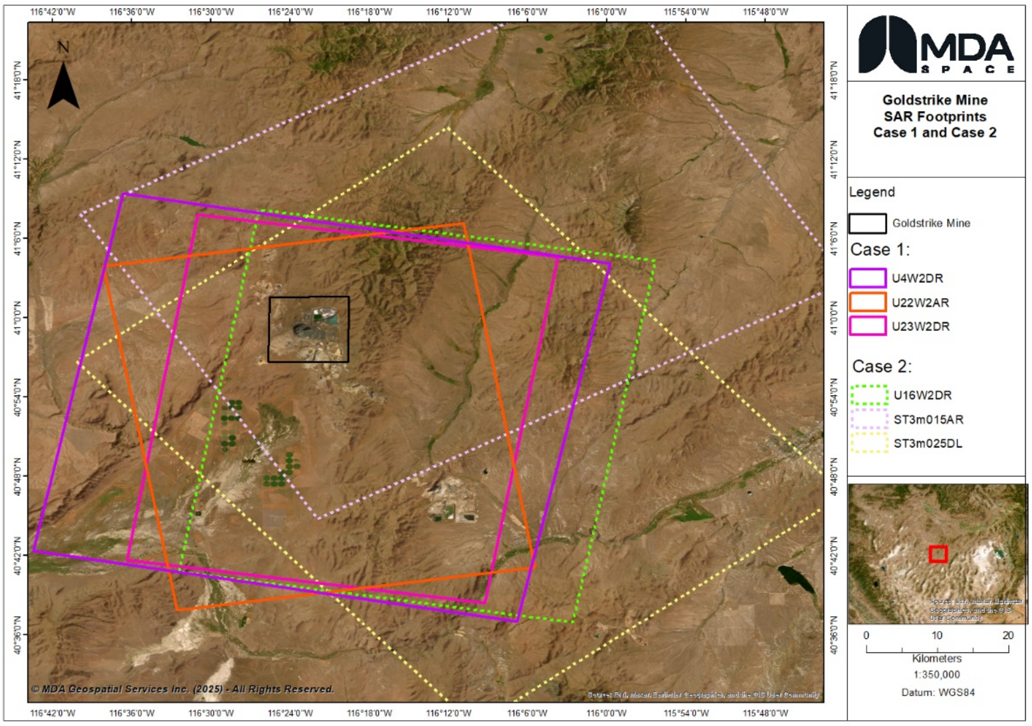

Figure 4 Goldstrike mine area of interest with RADARSAT-2 and CHORUS-C swath extents

2.3 Simulations

To represent the potential deformation that could occur at Betze-Post open pit, a simple deformation model was created. In this model any slope greater than 5° throughout the AOI was assigned a deformation rate of 5 mm/year in the downslope direction. The downslope direction is a vector defined independently for each pixel in the DEM by the aspect and slope. The aspect is the azimuth angle of the slope face, and the slope is the inclination angle with respect to the horizontal plane. The east–west, north–south and vertical components of this simulated deformation were calculated for each pixel. Figure 5 shows the simulated deformation components for the Goldstrike mine, focused on the Betze-Post open pit.

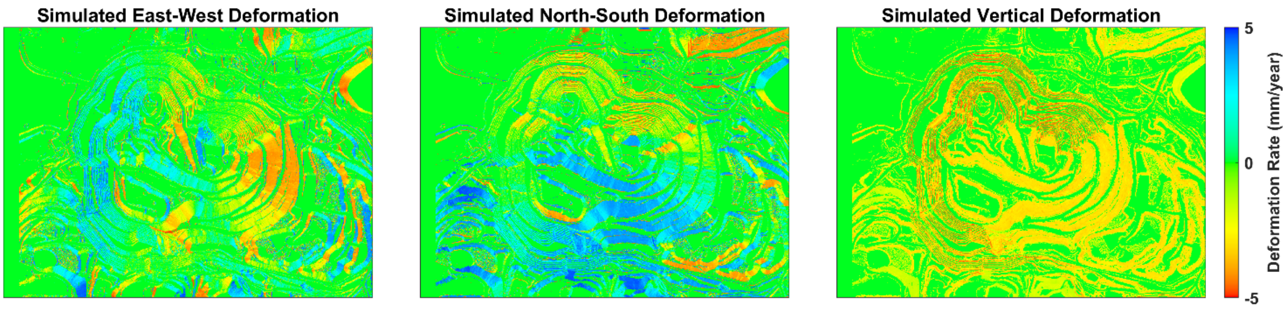

Figure 5 Simulated 3D surface displacement for the Betze-Post open pit

The simulated downslope deformation rate was projected to the LOS vector for each SAR beam from Table 2 to compute the LOS deformation rate measured by each. Additive noise of 0.5 mm/year was incorporated to each LOS measurement to investigate the numerical stability of 3D decomposition solutions. The residual between the LOS deformation and simulated deformation was calculated.

Separate 3D decompositions of the LOS InSAR measurements were carried out for Cases 1 and 2 to simulate how well the 3D surface displacement would be captured in either scenario. Additional simulations were performed to identify pixels in the AOI obscured by SAR image distortions. To do this, the local incidence angle for each pixel in the analysed region was calculated from the DEM and orbital parameters. Thresholding these local incidence angles indicates which pixels are in shadow or layover when imaged by any SAR beam. A more detailed analysis considering foreshortening will be the focus of future work. 3D decomposition is limited to pixels unobscured by shadow and layover in at least three independent InSAR image stacks. However, valid pixels in any one independent InSAR image stack still provide valuable LOS deformation information.

3 Results

In this section the simulated LOS InSAR deformation, 3D decompositions, and shadow and layover estimation for Cases 1 and 2 are presented

3.1 Line-of-sight Interferometric synthetic aperture radar deformation

The LOS deformation rate simulations for the three beams in Case 1 are shown in Figure 6. The arrows indicate the azimuth and range direction during image acquisition. This Figure shows that the sensitivity of the LOS InSAR measurements is strongly dependent on the orientation of the surface displacement vector with respect to the LOS; the lowest residuals are seen on slope aspects close to parallel with the range direction, and highest residuals are observed on surfaces sloping perpendicular to the range direction. SSO SAR sensors, such as RADARSAT-2, are more sensitive to horizontal surface displacement in the east–west plane as opposed to the north–south plane.

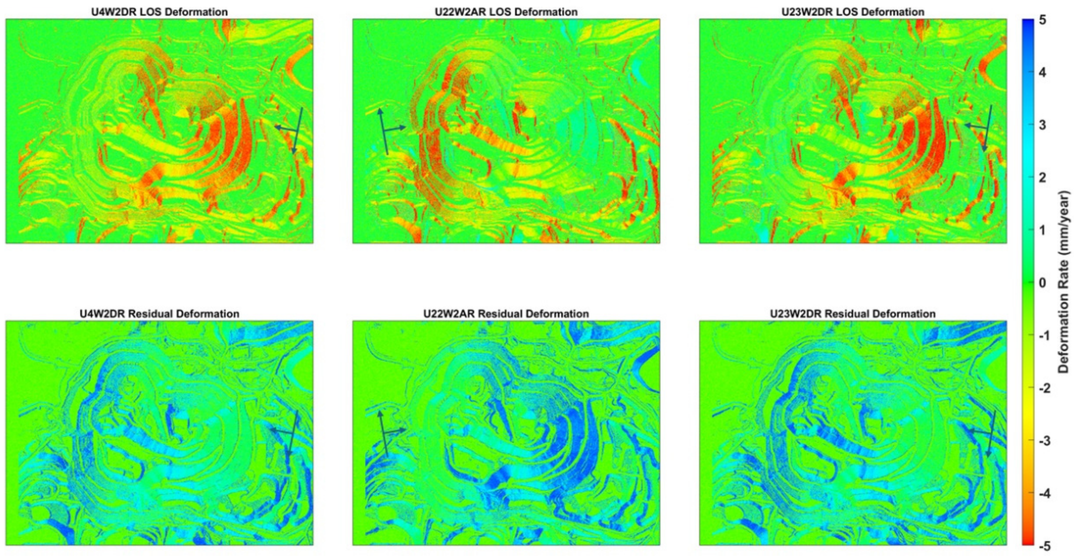

Figure 6 Simulated line-of-sight (LOS) deformation rate for the RADARSAT-2 beams in Case 1 (top row), and residual deformation between the LOS deformation rate and the simulated deformation

The LOS deformation rate simulations for the three beams in Case 2 are shown in Figure 7. Arrows indicate azimuth and range direction during image acquisition. In a similar manner to Case 1, the sensitivity of the LOS InSAR measurements is strongly dependent on the orientation of the surface displacement vector with respect to the LOS. However, in contrast to Case 1, there is no section of the pit that has high residuals in all observations.

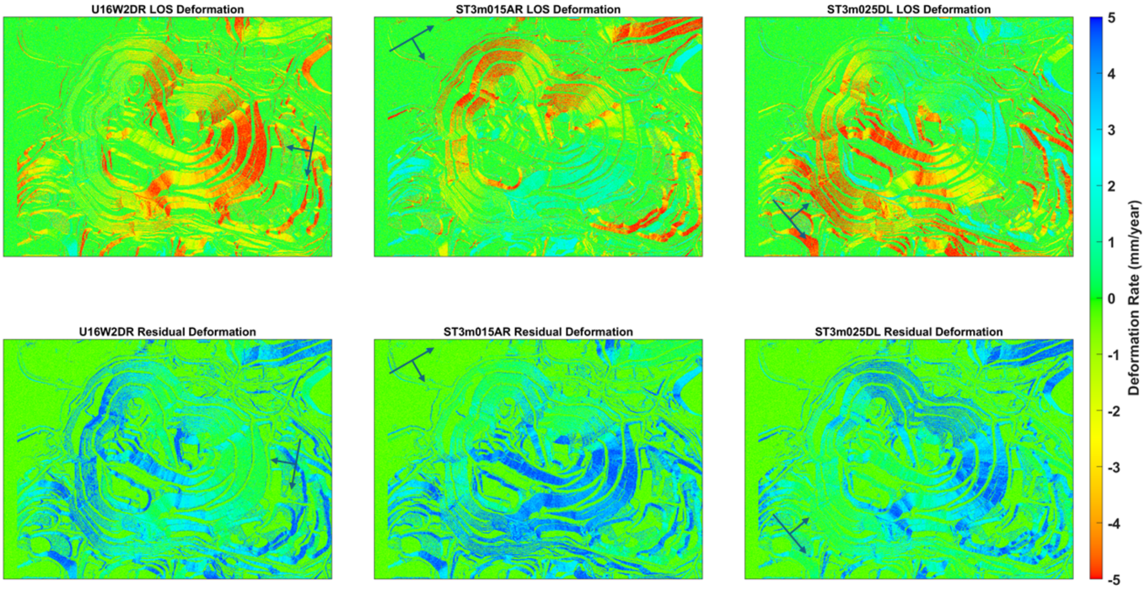

Figure 7 Simulated line-of-sight (LOS) deformation rate for the RADARSAT-2 and CHORUS-C beams in Case 2 (top row), and residual deformation between the LOS deformation rate and the simulated deformation

Figure 8 summarises these observations. The leftmost column indicates pixels where deformation was simulated. The middle column indicates the areas in which no meaningful LOS measurement (or even indication of deformation) can be made for Case 1 (top row) and Case 2 (bottom row). Similarly, the column on the right indicates the areas in which strong indications of deformation could be detected. These masks were made by thresholding the residual LOS deformation presented in Figures 7 and 8.

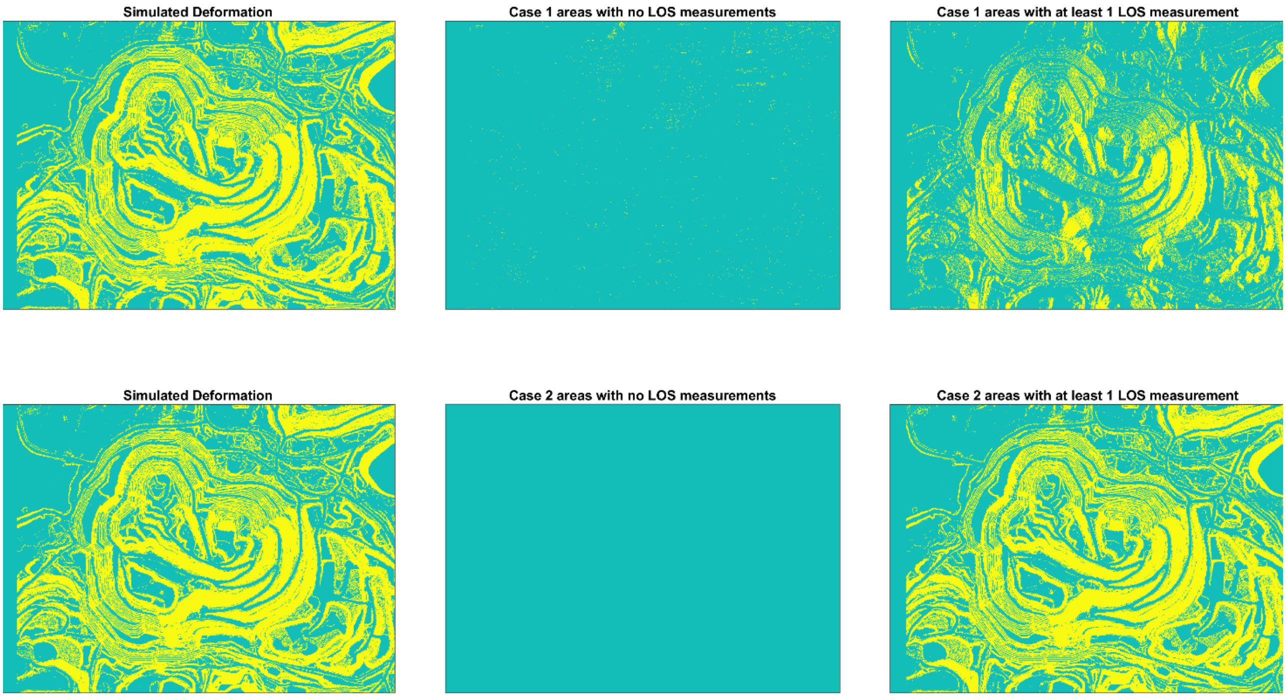

Figure 8 Areas available for line-of-sight (LOS) monitoring for Case 1 (top row) and Case 2 (bottom row)

3.2 3D decomposition

Figure 9 presents the simulated 3D decomposition results for the three RADARSAT-2 Ultrafine beams in Case 1.

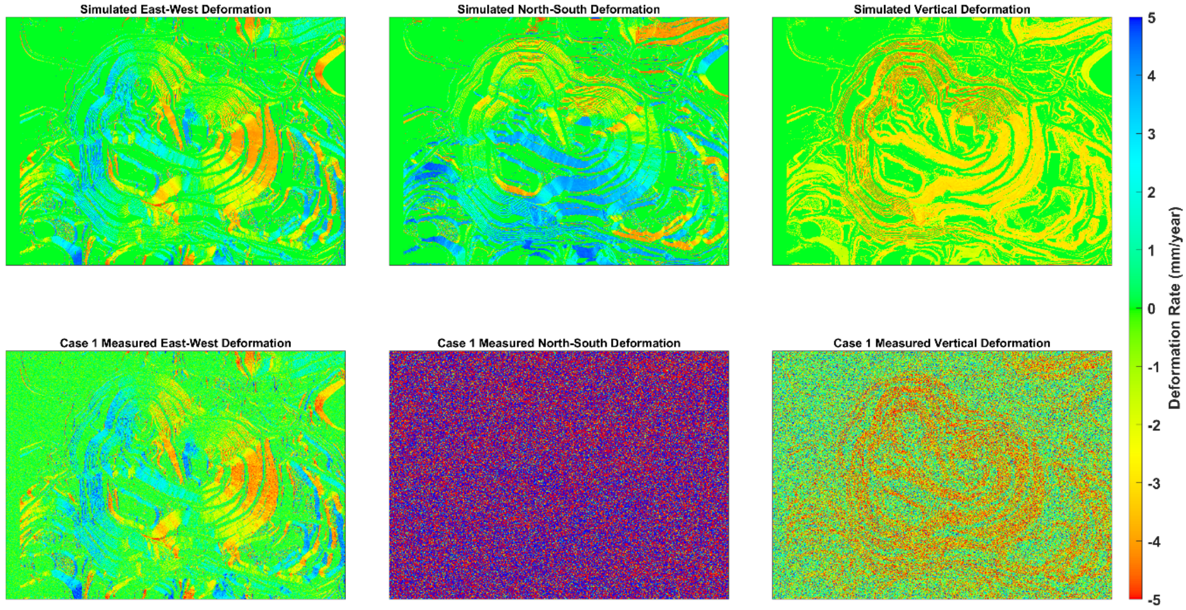

Figure 9 Simulated east–west, north–south and vertical deformation rate components (top row) and corresponding 3D decomposed deformation rates using the line-of-sight InSAR measurements for Case 1 (bottom row)

Figure 10 presents the simulated 3D decomposition results for combination RADARSAT-2 Ultrafine and CHORUS Stripmap beams in Case 2.

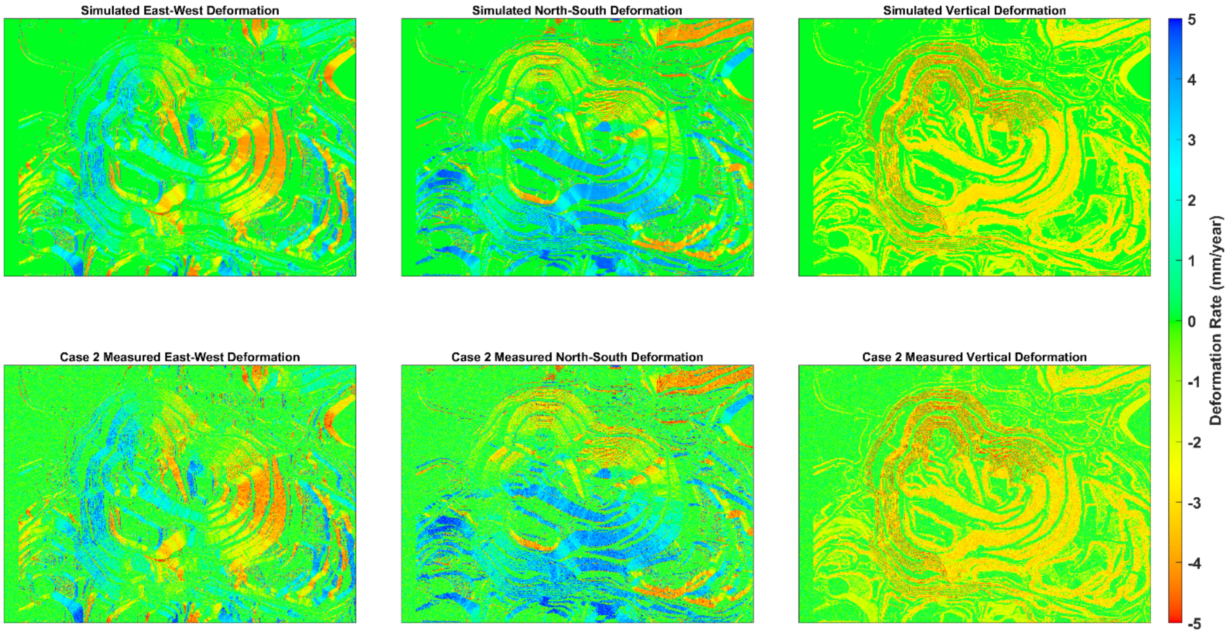

Figure 10 Simulated east–west, north–south and vertical deformation rate components (top row) and corresponding 3D decomposed deformation rates using the line-of-sight InSAR measurements for Case 2 (bottom row)

Figure 11 shows the residuals between the magnitude of surface displacement obtained by 3D decomposition in Cases 1 and 2 and the simulated deformation. Note that the colour scale has been reduced from ± 5 mm/year to ± 3 mm/year to better highlight the differences in the results.

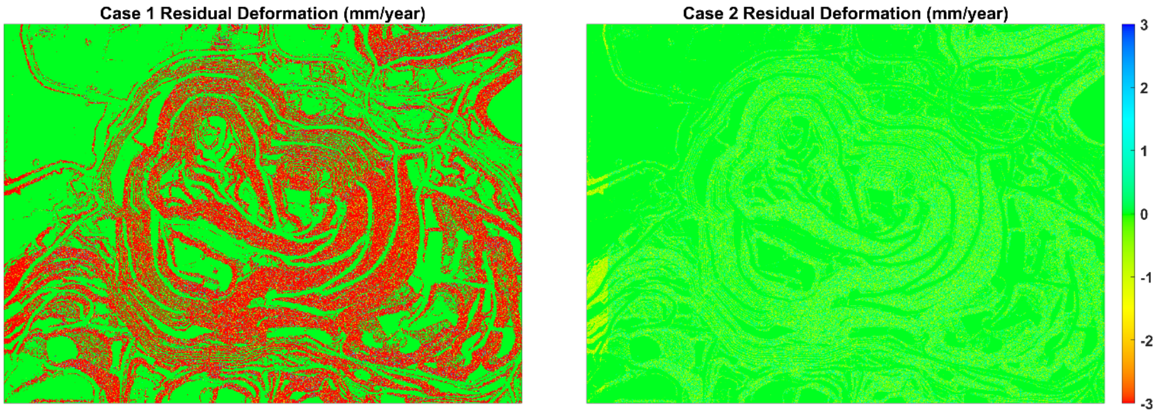

Figure 11 Residuals between the magnitude of the 3D decomposed surface displacement measurements in Cases 1 and 2 with the simulated deformation

3.3 Shadow and layover estimation

Figure 12 shows the combined shadow and layover masks for the beam combinations considered in Cases 1 and 2. These masks show pixels that would be obscured in at least one SAR image footprint from the different beams comprising either case due to SAR layover or shadow and represent the area in which no 3D decomposition can be performed. In Case 1, in which only RADARSAT-2 beams were considered, the layover and shadow regions overlap and cluster on the east and west faces. For Case 2, the main contribution to SAR image distortion is the shadows introduced from the ST3m025DL beam, which has a 62° incidence angle. The ST3m015AR beam has a somewhat smaller incidence angle, reducing the proportion of shadow compared to ST3m025DL and U16W2DR, however, the larger angular diversity of LOS in Case 2 means there is less overlap between these zones.

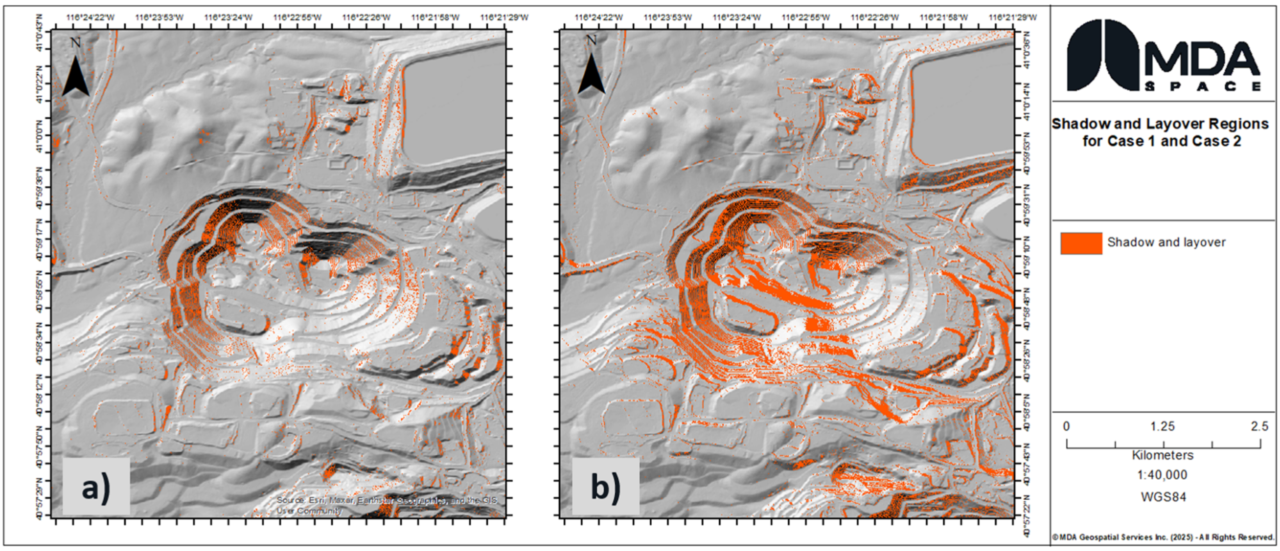

Figure 12 Synthetic aperture radar image distortion masks indicating pixels obscured by layover and shadow from the combined line-of-sight viewing geometries of beams considered in (a) Case 1 and (b) Case 2

4 Discussion

In this study, simulations were performed which demonstrate that the magnitude of surface displacement will typically be underestimated by single LOS InSAR measurements. Since the proportion of total deformation captured by each unique RADARSAT-2 or CHORUS beam is dependent on the alignment of the SAR LOS vector with the surface displacement, no individual LOS measurement, regardless of sensor, can fully measure the simulated downslope deformation in all areas of the AOI. However, separately analysing the LOS InSAR from each of the three beam modes provides some level of indication of surface displacement over a broader range of slopes than is possible with any single beam mode.

The simulation results presented in this study demonstrate that the precision in the reconstructed 3D components of surface deformation is significantly improved when LOS InSAR from CHORUS is incorporated into a monitoring plan with another SSO sensor. In Case 1, which only uses images from RADARSAT-2 (representing limitations from SSO SAR sensors), we see a representative reconstruction of the east–west deformation, which highlights the fact that these sensors have LOS vectors closely aligned with the east–west plane. There is virtually no sensitivity to reconstructing the north–south deformation component and the decomposition is highly unstable in this component. The vertical deformation component is poorly captured due to the limited angular diversity in the right-looking beam modes, which are similarly observed in Wright et al. 2004. In Case 2, which incorporates carefully selected CHORUS-C images, improved reconstruction of all 3D surface displacement components was demonstrated. The increased angular diversity provided by the CHORUS-C beams results in a stable solution that is much more robust to noise.

Full 3D decomposition requires at least three LOS InSAR measurements which are unobscured by SAR distortions, and in areas of steep topography this can limit the coverage areas available for decompositions. Figure 12 presents indications of the regions that would be excluded from decomposition for Cases 1 and 2. In Case 1, the contributions of shadow and layover tend to overlap for beams with opposing looks but similar incidence angles (i.e. the shadow of U22W2AR excludes similar regions as the foreshortening of U23W2DR and vice versa). For Case 2, each LOS vector introduces a unique contribution, with less overlap between them, which leads to a more dispersed set of excluded pixels. However, when only considering LOS InSAR measurements, the set of pixels visible from at least one beam mode will increase measurement coverage with increased angular diversity, as demonstrated in Figure 8.

When increasing the number of SAR beam modes incorporated into an InSAR monitoring program, the greater redundancy in the decomposition provides noise suppression and the resulting 3D decomposition will generally be improved. Further, the unique SAR image distortions from each beam mode introduce the opportunity to increase coverage of 3D InSAR over the AOI by considering different beam combinations for each pixel. A comprehensive InSAR monitoring plan includes careful selection of beam modes that balance measurement coverage with 3D InSAR performance, given the unique characteristics of the AOI and requirements in surface displacement monitoring.

5 Conclusion

This study provided a demonstration of how MDA Space’s upcoming MDA CHORUS synthetic aperture radar (SAR) constellation mission will provide enhanced InSAR monitoring capabilities in support of safe mining operations. The innovative mid-inclination orbit of CHORUS will provide unique viewing geometries that, when complemented by InSAR perspectives from existing SSO SAR sensors, will enable precise 3D decomposition of measurements to retrieve the full surface displacement vectors, including the north–south component in long-term displacement monitoring for the first time. This was illustrated by simulating downslope surface deformation at the Betze-Post open pit in Nevada, USA. The results show how CHORUS-C improves the ability to reconstruct 3D surface displacement from independent InSAR measurements from different SAR beams while also maximising the area available for monitoring with LOS InSAR. This improved InSAR capability can be incorporated into geotechnical monitoring programs to maximise the potential of SAR technology to support safe mining operations.

References

Brouwer, WS & Hanssen, RF 2023, ‘A treatise on InSAR geometry and 3-D displacement estimation’, *IEEE Transactions on Geoscience and Remote Sensing*, vol. 61, pp. 1–11.

Eppler, J, Mantle, V, Sharma, J & Caves, R 2023, ‘CHORUS SAR constellation: a mission capability overview’, *12th International Workshop on Advances in the Science and Applications of SAR Interferometry and Sentinel-1 InSAR – FRINGE 2023*,University of Leeds, Leeds.

Furhmann, T & Garthwaite, MC 2019, 'Resolving three-dimensional surface motion with InSAR: constraints from multi-geometry data fusion', *Remote Sensing*, vol. 11, no. 3, pp. 1–22.

Greene Gondi, F, Eppler, J, Caves, R & MDA CHORUS Team 2023, 'Enabling 3D deformation monitoring with the CHORUS SAR constellation'', *12th International Workshop on Advances in the Science and Applications of SAR Interferometry and Sentinel-1 InSAR – FRINGE 2023*,University of Leeds, Leeds.

Sharma, J & Caves, R 2022, 'CHORUS – changing how and when we observe our planet', *EUSAR 2022: 14th European Conference on Synthetic Aperture Radar*, VDE, Berlin, pp. 1–4.

Sharma, J, Caves, R & Mantle, V 2024, 'CHORUS mission update', *EUSAR 2024: 15th European Conference on Synthetic Aperture Radar*, VDE, Berlin, pp. 1008–1011.

Wright, TJ, Parsons, BE & Lu, Z 2004, 'Toward mapping surface deformation in three dimensions using InSAR', *Geophysical Research Letters*, vol. 31, no. 1, pp. 1–5.